Received: 13 March 2018 | Revised: 4 December 2018 | Accepted: 10 December 2018

DOI: 10.1111/fwb.13258



ORIGINAL ARTICLE

WILEY Freshwater Biology

# Responses of microbial activity in hyporheic pore water to biogeochemical changes in a drying headwater stream

Astrid Harjung[1,2] | Núria Perujo[3] | Andrea Butturini[4] | Anna M. Romaní[3] | Francesc Sabater[4,5]

[1]Department of Limnology and Bio-Oceanography, University of Vienna, Vienna, Austria

[2]WasserCluster Lunz Biologische Station GmbH, Lunz am See, Austria

[3]Institut d'Ecologia Aquàtica, Universitat de Girona, Girona, Spain

[4]Department Biologia Evolutiva, Ecologia i Ciències Ambientals, Fac. Biologia, Universitat de Barcelona, Barcelona, Spain

[5]Centre de Recerca Ecològica i Aplicacions Forestals (CREAF), Cerdanyola del Vallès, Spain

**Correspondence**
Astrid Harjung, Department of Limnology and Bio-Oceanography, University of Vienna, Vienna, Austria.
Email: astrid.harjung@univie.ac.at

**Funding information**
FP7 People: Marie-Curie Actions, Grant/Award Number: 607150; FP7 Environment, Grant/Award Number: 603629-ENV-6.2.1

## Abstract

1. Microbial heterotrophic activity is a major driver of nutrient and organic matter processing in the hyporheic zone of headwater streams. Additionally, the hyporheic zone might provide refuge for microbes when surface flow ceases during drought events.
2. We investigated chemical (organic and inorganic nutrients) and microbiological parameters (bacterial cell concentration, live–dead ratios, and extracellular enzyme activities) of surface and interstitial pore water in a period of progressive surface-hyporheic disconnection due to summer drying. The special situation of the chosen study reach, where groundwater mixing is impeded by the bedrock forming a natural channel filled with sediment, allowed as to study the transformation of these parameters along hyporheic flow paths.
3. The chemical composition of the hyporheic pore water reflected the connectivity with the surface water, as expressed in the availability of nitrate and oxygen. Conversely, microbiological parameters in all hyporheic locations were different from the surface waters, suggesting that the microbial activity in the water changes rapidly once the water enters the hyporheic zone. This feature was principally manifested in higher live–dead ratios and lower leucine aminopeptidase (an activity related to nitrogen acquisition) in the hyporheic pore waters.
4. Overall, bacterial cell concentration and extracellular enzyme activities increased along hyporheic flow paths, with a congruent decrease in inorganic nutrients and dissolved organic matter quantity and apparent molecular size.
5. Our findings show two important functions of the hyporheic zone during drought: (1) deeper (−50 cm) water-saturated layers can act as a refuge for microbial activity; and (2) the hyporheic zone shows high rates of carbon and nitrogen turnover when water residence times are longer during drought. These rates might be even enhanced by an increase in living microbes in the remaining moist locations of the hyporheic zone.

KEYWORDS

dissolved organic matter processing, extracellular enzyme activities, hyporheic zone, intermittent stream, live-dead ratio

## 1 | INTRODUCTION

From a hydrological perspective, the hyporheic zone is defined as the sediments, where stream water enters the subsurface and returns to the stream channel at the reach scale (Wondzell & Gooseff, 2013). From an ecological perspective, the hyporheic zone is a biogeochemical hot spot with high turnover rates of organic matter and inorganic nutrients, because most of microbial heterotrophic activity occurs in this compartment (Boulton, Findlay, Marmonier, Stanley, & Valett, 1998; Danczak et al., 2016; McClain et al., 2003). For instance, hyporheic denitrification can comprise up to twice the rate of whole stream (benthic and pelagic) denitrification (Harvey, Böhlke, Voytek, Scott, & Tobias, 2013) and the biggest portion of dissolved organic matter (DOM) is metabolised there (Naegeli & Uehlinger, 1997; Rasilo, Hutchins, Ruiz-González, & del Giorgio, 2017). Principal drivers of the rates and types of metabolic processes occurring in the hyporheic zone are hydrological exchange and discharge, because these drivers determine the length and water residence time of hyporheic flow paths (Boulton, Datry, Kasahara, Mutz, & Stanford, 2010). Similarly, various studies report differences in dissolved oxygen concentration and nitrogen removal between up- and downwelling locations, with downwelling sites as hot spots of nitrification (Edwardson, Bowden, Dahm, & Morrice, 2003; Storey, Williams, & Fulthorpe, 2004; Triska, Duff, & Avanzino, 1990). The physicochemical gradients along hyporheic flow paths are steep and, at the same time, disturbances at the surface are buffered (Krause et al., 2011). Hence, the hyporheic zone of intermittent streams might serve as a refuge for microbes, when surface flow ceases in the course of annual summer droughts (Romaní et al., 2013). In the light of today's pressures on fluvial ecosystems that enclose water abstraction and changes in precipitation regime due to global warming (Pachauri et al., 2014), it is imperative to understand hydrological and biogeochemical constraints on microbial activity across the surface–hyporheic interface.

Microbial activity has been found to be related to DOM content of the sediment (Eiler, Langenheder, Bertilsson, & Tranvik, 2003; Fischer, Sachse, Steinberg, & Pusch, 2002) whereby the source and lability of DOM play a key role for microbial metabolism (Chafiq, Gibert, & Claret, 1999; Hall & Tank, 2003). Leachates from microbial assemblages provides an autochthonous DOM source that is assumed to be even more labile for microbes (Anesio, Granéli, Aiken, Kieber, & Mopper, 2005). Allochthonous DOM is typically considered resistant to microbial metabolism. However, in highly oligotrophic systems the quantity of allochthonous DOM has shown to drive shifts in community composition (Eiler et al., 2003). By contrast, autochthonous DOM has been found to affect community composition only transiently (Wagner et al., 2014). Additionally, the mixture of fresh labile and accumulated refractory DOM that naturally occurs in aquatic ecosystems could accelerate bacterial growth and bacterial DOM removal (Farjalla et al., 2009).

So far, the responses of microbial activity to specific environmental conditions, such as desiccation, oxygen distribution or temperature, have been mainly investigated under laboratory conditions in sand filtration columns or in mesocosm experiments with streambed sediment (Amalfitano et al., 2008; Freixa, Rubol, et al., 2016; Liu et al., 2017; Perujo, Sanchez-Vila, Proia, & Romaní, 2017). While these experiments target only one or two of the physical or chemical factors that potentially drive microbial activity, we expected that the microbial activity in streams is driven by a whole set of environmental conditions (Arce, del Mar Sánchez-Montoya, Rosario Vidal-Abarca, Suárez, & Gómez, 2014; Zhu & Dittrich, 2016). These environmental conditions are even more heterogeneous during the drying period of an intermittent stream (Febria, Beddoes, Fulthorpe, & Williams, 2012). This set of microhabitats at the surface and subsurface is subjected to rapid biogeochemical changes that determine microbial activity (Lake, 2003; Vervier, Dobson, & Pinay, 1993). For instance, the DOM composition and inorganic nutrient availability undergo severe changes during the drying of an intermittent stream (Gómez, García, Vidal-Abarca, & Suárez, 2009; Vázquez, Amalfitano, Fazi, & Butturini, 2011). Based on prior research carried out at the intermittent study site, we had selected a reach where the hyporheic zone was confined by impermeable bed rock and, therefore, impeding groundwater mixing (Harjung, Sabater, & Butturini, 2017). This situation excluded groundwater as a potential end-member and offered the possibility to investigate the hyporheic zone as a biogeochemical reactor driving dissolved organic carbon (DOC) and inorganic nutrient retention and release, as well as DOM quality changes.

In the present study, we linked chemical changes to the bacterial cell concentration, live–dead ratio and extracellular enzyme activities. We expected that the microbes will survive and might even proliferate in the hyporheic zone, as the hyporheic zone represents a refuge when surface flow ceases. The living bacteria accumulated at the hyporheic pore water may maintain key functions for nutrient and carbon cycling that are reduced at the drying surface. We focused on microbial activity in the interstitial pore water rather than attached to the sediment, because in the water, the responses to environmental changes will be observed immediately (Febria et al., 2012). The two specific objectives were: (1) to compare microbial activity and chemical parameters in surface and hyporheic pore water; and (2) to explore temporal variability of microbial activity along hyporheic flow paths and its relationship to increasing water residence times and changes in nutrient and energy availability. Our hypothesis was that DOM transformation is limited by availability of oxygen and nutrients when water progressively vanishes during the drought period. We further hypothesised that as surface flow ceases, microbiota survive in the hyporheic zone, where moisture permits maintenance of the microbial activity.

## 2 | METHODS

### 2.1 | Study site and sampling strategy

The Fuirosos stream is an intermittent headwater stream in the north-east of the Iberian Peninsula, with an underlying catchment geology comprised of leucogranite and granodiorit, draining off into

the Tordera river (Vazquez et al., 2013). The mean annual temperatures range from 3°C in January to 24°C in August (Butturini, Bernal, Sabater, & Sabater, 2002), and the average annual mean precipitation is exceeded by the average annual potential evapotranspiration (Medici et al., 2008). Baseflow ranges from 0 to 20 L/s (Butturini et al., 2003). The studied reach, located at the valley bottom of the Fuirosos catchment between 160 and 165 m above sea level (latitude 41° 42′23″-28″, longitude 2° 34′81″-86″) was chosen because the exposure to the surface of the bedrock interrupts the hyporheic zone that is composed of alluvial gravel (2–5 cm) with sand and fine sand fractions (for more information see Artigas, Romaní, Gaudes, Muñoz, & Sabater, 2009). The exposed bedrock channel is 63 m long, flanked by shallow sandy sediments and then covered again forming a channel of alluvial sediments of approximately 1–2 m depth. This sediment channel is supplied by surface water and during rainy periods by hillslope runoff but is cut off from groundwater supply by the bedrock formation. The hyporheic connectivity is restricted to surface flow by the uplift of the bedrock acting as a natural barrier. Due to the impermeability of the bedrock channel surface water is still captured in small pools (5–7 $m^3$) and in the hyporheic zone, even when there is no surface flow present above the alluvial sediments. The riparian vegetation along the study reach is not dense and hardly causing light limitation.

In a previous study, electrical conductivity and stable water isotopes were used to separate the hydrological phases and investigate the hydrological connectivity between the sampling locations (Harjung et al., 2017). We performed five samplings between June and September 2014 to follow the drying period. The first sampling (19 June) represented the pre-drought phase with a discharge of 6 L/s and the second sampling (3 July) exemplified the contraction phase with a discharge of 1.4 L/s. The contraction phase started when the water level in the pool dropped and showed a continuous decrease (Figure 1). The approximated water residence times for these two phases were estimated from salt slug injections, taking the time that electrical conductivity needed to recover to background values at the measuring point downstream. This tail of the salt tracer curve is indicative for the water volume having passed through the hyporheic zone. It was not possible to achieve a similar estimation for the later samplings. However, the absence of diurnal temperature cycles in the hyporheic zone downstream indicated that water residence time exceeded 24 hr. The reason for this is that the longer the water travels through the hyporheic zone, the more the diurnal temperature cycles of the surface water will be dampened. The third sampling on 17 July, with a discharge of 0.07 L/s, represented the transition phase from contraction to fragmentation. The fourth sampling (28 July with a discharge of 0.05 L/s) was performed during the fragmentation phase, which is characterised by the absence of surface water at the permeable streambed upstream and the hydrological disconnection of the hyporheic zone up-and downstream the bedrock. Finally, the fifth sampling (3 September with a discharge of 0 L/s) was performed during the dry phase, when the surface water was absent along the whole reach, with the exception of the pools in the impermeable zones. The interstitial pore water of the hyporheic zone was pumped with a peristaltic pump from PVC tubes that were perforated over 30 cm on the bottom and were installed at a depth of 50 cm in the hyporheic zone. The sampling locations included an upstream well ($HZ_{up}$) two lateral wells ($HZ_{lat1}$, $HZ_{lat2}$) and two wells downstream of the pool ($HZ_{inf}$, $HZ_{dw}$, Figure 1). The well

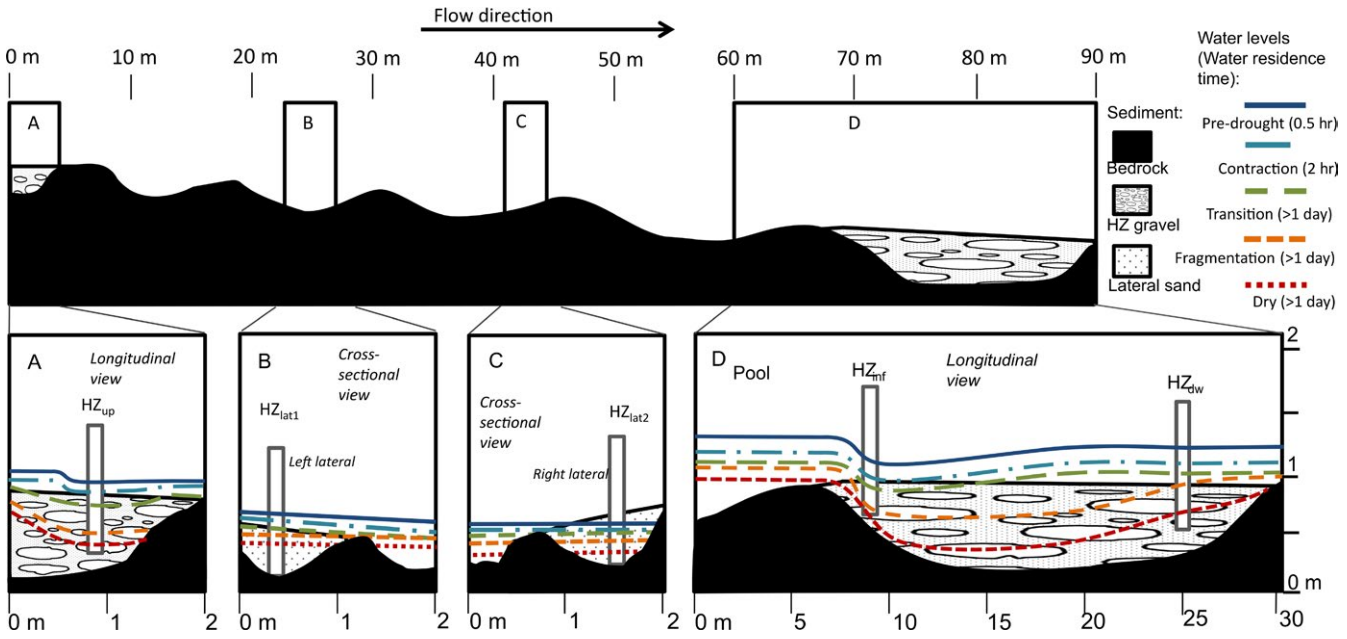


**FIGURE 1** Scheme of stream reach, where the top panel is an overview of the complete sampled reach together with the legend for the subsurface type on the right and the individual panels on the bottom represent the magnification of geomorphologic situation of the sampling locations. The coloured and differently dashed lines indicate the approximate water level of each phase. Panels a and d show the longitudinal view, while panels b and c present cross-sectional views [Colour figure can be viewed at wileyonlinelibrary.com]

$HZ_{up}$ was located upstream of the bedrock and was characterised by downwelling during flow conditions. The two wells at the lateral of the main channel were located in the sandy sediments flanking the bedrock channel. $HZ_{lat1}$ was located at the riparian zone next to the bedrock structure on the left side receiving water from the hillslope, and $HZ_{lat2}$ was located on the right lateral receiving mainly surface water from the bedrock channel. The most downstream of the pools mentioned previously served as a reference for the water entering the hyporheic zone channel. $HZ_{inf}$ refers to the well directly downstream of the pool, where the water of the pool infiltrated into the hyporheic zone. The well $HZ_{dw}$ was located 25 m downstream of the pool and was subjected to upwelling.

Dissolved oxygen was measured using an YSI 20 Pro oxygen sensor probe inside the wells immediately after pumping and was deployed in the pool and $HZ_{dw}$ to obtain continuous dissolved oxygen and temperature measurements. Surface and interstitial water samples for microbiological analyses were either incubated in the field for the measurement of extracellular enzyme activities, or placed in sterile vials and fixed for bacterial cell concentration and viability taking three replicates at each location (see below). Both surface and interstitial pore water samples for chemical analyses were filtered with ashed GF/F filters 0.7-μm nominal pore size, and then electrical conductivity (WTW Cond 3310 Conductivity meter) and pH (Thermo Scientific Orion Star A121 pH meter) were measured. Samples for laboratory analysis were collected in pre-washed (MilliQ) polyethylene bottles (one sample per location and sampling). The samples for inorganic nutrient concentration and DOM optical properties were filtered through 0.2-μm nylon filters, and the samples for DOC analysis were acidified with 10% HCl. All samples were stored at 4°C temperature in the dark and analysed within a week.

## 2.2 | Microbiological analysis

Extracellular enzyme activities β-glucosidase (EC 3.2.1.21), cellobiohydrolase (EC 3.2.1.91), phosphatase (EC 3.1.3.1-2), and leucine aminopeptidase (EC 3.4.11.1) were measured spectrofluorometrically using fluorescent-linked artificial substrates (methylumbelliferyl [MUF]-β-D-glucopyranoside, MUF-cellobioside, MUF-phosphate and L-leucine-7-amido-4-methylcoumarin hydrochloride [AMC]; Sigma-Aldrich). All enzyme activities were measured under saturating conditions (0.3 mM for β-glucosidase, phosphatase, and leucine aminopeptidase (Romaní & Sabater, 2000); and 0.9 mM for cellobiohydrolase (Mora-Gómez, Duarte, Cássio, Pascoal, & Romaní, 2018). Water samples (4 ml) were placed in falcon tubes, and artificial substrates were added for the determination of extracellular activities (120 μl for β-glucosidase, phosphatase, and leucine aminopeptidase and 400 μl for cellobiohydrolase determination). A blank for each artificial substrate with MilliQ water was prepared in order to determine the abiotic hydrolysis of the substrate itself. Samples and blanks were incubated in the field for 1 hr in the dark maintaining the same temperature as in the field by placing a tube rack immersed in the stream water. After a 1-hr incubation, glycine buffer (4 ml, pH 10.4) was added at each sample in order to stop the reaction and maximise MUF and AMC fluorescence. Samples were kept cold and transported to the laboratory for fluorescence readings. Aliquots (350 μl) of each sample were placed into wells of a 96-well black plate (Greiner bio-one). Fluorescence was measured at an excitation/emission (ex/em) wavelength of 365/455 (MUF fluorescence) and 364/445 (AMC fluorescence) in a fluorimeter plate reader (Tecan, infinite M200 Pro). To determine extracellular enzyme activities, MUF and AMC standards were prepared and measured for their fluorescence. Results are given in nmol MUF $ml^{-1}$ $hr^{-1}$ or nmol AMC $ml^{-1}$ $hr^{-1}$.

Bacterial cell concentration was determined by flow cytometry as described below, adapted from Amalfitano and Fazi (2008). Water samples (1 ml) were placed in sterilised glass vials, and detaching solution (9 ml) was added to each water sample. Detaching solution consisted of NaCl (130 mM), $Na_2HPO_4$ (7 mM), $NaH_2PO_4$ (3 mM), formaldehyde (37%), sodium pyrophosphate decahydrate 99% (0.1% final concentration), and Tween 20 (0.5% final concentration), which fixes the sample and helps in avoiding bacterial aggregates. Samples were vortexed, and an aliquot (400 μl) of each sample was stained with Syto 13 (4 μl Fisher, 5 μM), and incubated in the dark for 15 min. To calculate bacterial cell concentration, an internal standard (10 μl of beads solution $10^6$ beads/ml, Fisher, 1.0 μm) was added to each sample. Bacterial cell concentration was measured by flow cytometry (FACSCalibur, Becton–Dickinson). Results are reported as bacteria cells/ml.

Bacterial viability was determined by microscope counting. Water samples (2 ml) were stained (3 μl) using the Live/Dead BacLight Bacterial Viability Kit, which includes Syto 9 and propidium iodide stains. Samples were incubated for 15 min in the dark. Samples were filtrated (black polycarbonate filter, 0.2 μm), and each filter was prepared for counting in an epifluorescence microscope (Nikon E 600 at 1,000× magnification). Syto 9 penetrates all bacterial membranes and stains the cells fluorescent green, while propidium iodide only penetrates cells with damaged membranes, and the combination of the two stains produces red fluorescing cells (Boulos, Prévost, Barbeau, Coallier, & Desjardins, 1999). Results are presented as the ratio of the counted live cells (in green) to the counted dead ones (in red; live–dead ratio).

## 2.3 | Nutrient analysis

All water samples were analysed for ammonium ($NH_4$), nitrate ($NO_3$), soluble reactive phosphorus (SRP), and DOC concentrations, as well as DOM optical properties. Dissolved organic carbon concentrations were measured with the high-temperature catalytic oxidation method (Shimadzu TOC analyser). $NO_3$ was measured using the cadmium reduction method (Keeney & Nelson, 1982) with a Technicon Autoanalyzer. SRP and $NH_4$ were measured using a Shimadzu UV-2401 UV-Vis spectrophotometer using the molybdate method of Murphy and Riley (1962) for SRP and the salicylate method described by Reardon (1966) for $NH_4^+$. The samples for DOM optical properties were analysed at room temperature. Absorbance measurements

were conducted using a 1-cm path length cell with the same spectrophotometer over a wavelength range of 200–800 nm. Fluorescence was measured with a Shimadzu RF-5301PC spectrofluorometer over (ex/em) wavelengths of 240–420 nm and 280–690 nm respectively using a 1-cm path length cell.

### 2.4 | DOM quality indices

All DOM data treatment was performed with MATLAB (version R2015b, MathWorks). The raw fluorescence data were divided by a correction file obtained for the lamp in use following the protocol of (Gardecki & Maroncelli, 1998) and then normalised to the Raman area to account for lamp decay over time (Lawaetz & Stedmon, 2008). Absorbance data of the respective samples were used to correct for the inner-filter effect (Lakowicz, 2006). MilliQ water blanks were subtracted to remove Raman scattering (Goletz et al., 2011). Excitation–emission matrices were generated over (ex/em) wavelengths of 240–420 nm and 280–690 nm, respectively. Excitation at 370 nm was used to calculate the fluorescence index values from the ratio of intensities emitted at 470:520 nm (Cory & McKnight, 2005), whereby lower values indicate terrestrial origin and higher values correspond to autochthonous DOM (McKnight et al., 2001). Biological index describes freshness (higher values refer to more recent production) and biological activity as origin of DOM (Huguet et al., 2009). We applied this index taking the ratio of 380 nm and 430 nm from the excitation spectra at 310 nm. The humification index that increases with humification of DOM was calculated using the area under the em spectra 435–480 nm divided by the sum of the area under the em spectra 310–345 nm and 435–480 nm at ex 254 nm (modified from Ohno, 2002). Specific UV absorbance was computed as absorbance measured at 254 nm, normalised to the DOC concentration and reported in units of L $mg^{-1}$ $m^{-1}$. Higher specific UV absorbance at 254 nm has been found to correspond to higher aromaticity of DOM compounds (Weishaar et al., 2003). Spectral slope ratio was calculated as described by Helms et al. (2008), attributing an increase in this ratio to irradiation. The absorbance ratio $E_2E_3$, which is the ratio of absorbance at wavelength 250–365 nm, increases as molecular weight decreases (Peacock et al., 2014).

### 2.5 | Data analysis

For testing our first hypothesis regarding the differences between sampling locations, we used the following statistical tools. To assess if the location significantly affected water chemistry and microbial activity, a resemblance matrix based on the normalised Euclidean distance was calculated for a one-way analysis of similarity (ANOSIM), which calculates a global R statistic that assesses the differences in variability between groups compared to the variability within the group and checks for the significance of R using permutation tests. The ANOSIM was tested for the biogeochemical and the microbiological dataset separately and were tested for groups (1) sampling locations and (2) surface versus hyporheic. A canonical analysis of principal coordinates (CAP) was performed to visualise and classify the locations. CAP is a constrained ordination tool that discriminates locations defined a priori and determines the level of misclassification among sampling locations (Anderson & Willis, 2012). These features enabled us to determine which sampling locations were undergoing most changes and therefore reached highest misclassifications and which sampling locations showed stable conditions over time. Appropriate axis (m) was chosen by minimising the *p*-value from the permutation test based upon the trace statistic and maximising the leave-one-out allocation success, as suggested by Ratkowsky (2016). This approach tests how good the locations were discriminated using CAP. Furthermore, to quantify the effect of each variable to potential differences among locations, Spearman correlations were calculated for all variables and the CAP axes. Only the variables with a correlation coefficient $|r| > 0.4$ were considered. For both analyses, we used the PRIMER 6 + PERMANOVA (v. 6.1.11) computer program (Primer-E Ltd., Plymouth, UK) (Anderson, Gorley, & Clarke, 2008). The values were log(x + 1)-transformed to achieve normality. Additionally, one-way ANOVA with Tukey's *post hoc* analysis was used to evaluate differences between sampling locations at a significance level of $p < 0.01$.

Concentration differences along hyporheic flow paths were tested with a paired Student *t* test at a significance level of $p < 0.05$ for differences between pool and $HZ_{inf}$, as well as $HZ_{inf}$ and $HZ_{dw}$. To investigate if there is a correlation between increases/decreases along hyporheic flowpaths with drought, we calculated Spearman rank correlations between the percentage increase/decrease and the discharge. A redundancy analysis (RDA) using the R-package *vegan* (Oksanen et al., 2013) was performed, whereby the environmental biogeochemical conditions were explanatory variables for the microbiological variables. Pretreatment consisted in removing redundant environmental variables by checking for collinearity and Hellinger transformation of microbiological variables (Legendre & Gallagher, 2001). The function *envfit* was used to evaluate which biogeochemical variables were significantly correlated with the first two RDA axes ($p < 0.05$).

## 3 | RESULTS

### 3.1 | Physico-chemical characteristics and microbial activities across the surface–hyporheic pore water interface

Water physics and chemistry were characterised by electrical conductivity among 200–400 µS/cm, a pH between 6.5 and 7.2, 2–8 mg/L of DOC, and low nutrient content (Table 1). With regard to the microbiological parameters, the surface waters were characterised by higher β-glucosidase and leucine aminopeptidase, while the interstitial pore waters exhibited a higher live–dead ratio (see ANOVA results in Table 1).

Significant differences between locations were found for the chemical variables (Table 1, ANOSIM $R = 0.394$, $p < 0.001$) but surface water samples were not separated from the hyporheic pore

**TABLE 1** Mean ± standard deviation of all sampling locations (column) for all five samplings, when the location was not dry

| Variable | $HZ_{up}$ ($n$ = 5) | $HZ_{lat1}$ ($n$ = 5) | $HZ_{lat2}$ ($n$ = 5) | $HZ_{inf}$ ($n$ = 4) | $HZ_{dw}$ ($n$ = 5) | Pool ($n$ = 5) | Stream ($n$ = 7) |
|---|---|---|---|---|---|---|---|
| Bacteria*, $10^6$ cells/ml | **$5.9^{b} \pm 8.9$** | $1.1^{ab} \pm 0.3$ | $1.3^{ab} \pm 1.0$ | $0.4^{a} \pm 0.5$ | $1.1^{ab} \pm 0.7$ | $2.8^{ab} \pm 2.9$ | $0.6^{ab} \pm 0.1$ |
| Live–dead-ratio* | $0.41^{b} \pm 0.29$ | $0.22^{ab} \pm 0.13$ | $0.19^{ab} \pm 0.08$ | $0.69^{b} \pm 0.38$ | **$0.74^{b} \pm 0.4$** | $0.06^{a} \pm 0.06$ | $0.09^{ab} \pm 0.05$ |
| β-glucosidase*, nmol $ml^{-1}$ $hr^{-1}$ | $0.01^{a} \pm 0.00$ | $0.02^{a} \pm 0.02$ | $0.01^{a} \pm 0.01$ | $0.01^{a} \pm 0.01$ | $0.05^{a} \pm 0.05$ | **$0.08^{a} \pm 0.05$** | **$0.08^{a} \pm 0.03$** |
| Phosphatase, nmol $ml^{-1}$ $hr^{-1}$ | 0.42 ± 0.68 | 0.04 ± 0.06 | 0.07 ± 0.09 | 0.10 ± 0.09 | **0.31 ± 0.32** | 0.23 ± 0.18 | 0.15 ± 0.10 |
| Cellobiohydrolase, nmol $ml^{-1}$ $hr^{-1}$ | 0.00 ± 0.00 | 0.00 ± 0.00 | 0.00 ± 0.00 | 0.00 ± 0.00 | 0.00 ± 0.00 | 0.00 ± 0.00 | 0.01 ± 0.02 |
| Leucine-aminopeptidase*, nmol $ml^{-1}$ $hr^{-1}$ | $0.23^{ab} \pm 0.29$ | $0.03^{a} \pm 0.03$ | $0.19^{ab} \pm 0.12$ | $0.26^{ab} \pm 0.28$ | $0.27^{ab} \pm 0.33$ | **$0.82^{b} \pm 0.61$** | $0.76^{b} \pm 0.57$ |
| Fluorescence index | 1.52 ± 0.03 | **1.58 ± 0.03** | 1.53 ± 0.08 | 1.49 ± 0.01 | 1.53 ± 0.05 | 1.49 ± 0.01 | 1.50 ± 0.08 |
| Humification index* | $0.87^{a} \pm 0.03$ | **$0.95^{b} \pm 0.02$** | $0.91^{ab} \pm 0.02$ | $0.92^{ab} \pm 0.03$ | $0.89^{ab} \pm 0.02$ | $0.90^{ab} \pm 0.03$ | $0.91^{ab} \pm 0.02$ |
| Biological index | 0.58 ± 0.02 | 0.58 ± 0.01 | 0.59 ± 0.01 | 0.59 ± 0.01 | **0.60 ± 0.02** | 0.58 ± 0.02 | **0.60 ± 0.03** |
| Slope ratio | 1.01 ± 0.24 | 0.87 ± 0.07 | 0.95 ± 0.13 | **1.07 ± 0.31** | 1.06 ± 0.32 | 0.98 ± 0.19 | 0.94 ± 0.17 |
| Specific ultraviolet absorbance at 254 nm L mg-$C^{-1}$ $m^{-1}$ | 1.87 ± 0.58 | 2.05 ± 0.40 | **2.34 ± 0.28** | 2.06 ± 0.74 | 2.25 ± 0.25 | **2.34 ± 0.24** | 2.32 ± 0.35 |
| $E_2E_3$ (index molecular size) | 6.81 ± 0.63 | **7.23 ± 1.03** | 7.22 ± 0.89 | 5.98 ± 0.82 | 6.72 ± 1.20 | 5.73 ± 0.63 | 6.05 ± 0.57 |
| DOC, mg/L | 3.34 ± 1.54 | **5.15 ± 1.54** | 2.70 ± 0.57 | 3.08 ± 1.28 | 2.78 ± 0.50 | 3.17 ± 0.70 | 2.68 ± 0.42 |
| Dissolved oxygen*, mg/L | $1.25^{ab} \pm 0.46$ | $1.03^{ab} \pm 0.47$ | $2.49^{abc} \pm 1.37$ | $4.20^{abc} \pm 2.38$ | $0.91^{a} \pm 0.68$ | **$6.33^{c} \pm 1.75$** | $6.23^{bc} \pm 3.04$ |
| $NO_3$*, mg/L | $0.11^{a} \pm 0.07$ | $0.09^{a} \pm 0.05$ | $0.09^{a} \pm 0.06$ | **$0.71^{b} \pm 0.30$** | $0.23^{ab} \pm 0.15$ | $0.14^{ab} \pm 0.09$ | $0.15^{ab} \pm 0.09$ |
| SRP, µg/L | 18.08 ± 10.38 | 21.54 ± 1.85 | 14.61 ± 5.51 | **32.14 ± 8.20** | 21.54 ± 5.79 | 22.15 ± 9.27 | 23.4 ± 3.81 |
| $SO_4$*, mg/L | **$7.57^{b} \pm 4.93$** | $1.96^{a} \pm 1.03$ | $5.87^{b} \pm 1.16$ | $5.72^{b} \pm 0.46$ | $5.58^{b} \pm 0.55$ | $5.67^{b} \pm 0.55$ | $5.69^{b} \pm 0.40$ |
| $NH_4$* mg/L | $0.09^{bc} \pm 0.03$ | **$0.33^{d} \pm 0.10$** | $0.13^{cd} \pm 0.03$ | $0.03^{a} \pm 0.01$ | $0.09^{abc} \pm 0.08$ | $0.04^{ab} \pm 0.02$ | $0.03^{ab} \pm 0.01$ |
| pH* | **$7.02^{b} \pm 0.16$** | $6.55^{a} \pm 0.10$ | $6.75^{ab} \pm 0.12$ | $6.97^{b} \pm 0.13$ | $6.92^{b} \pm 0.15$ | $6.98^{b} \pm 0.14$ | $6.99^{b} \pm 0.10$ |
| Temperature, °C | 20.0 ± 1.9 | 19.8 ± 1.7 | 20.0 ± 1.8 | 20.2 ± 2.3 | 21.0 ± 1.9 | **21.3 ± 3.3** | 20.8 ± 3.3 |
| Electrical conductivity*, µS/cm | $289^{ab} \pm 64$ | **$398^{b} \pm 23$** | $280^{ab} \pm 31$ | $259^{a} \pm 28$ | $274^{a} \pm 45$ | $275^{a} \pm 48$ | $251^{a} \pm 23$ |

Asterisks next to the variables highlight significant differences between sampling locations detected with the one-way ANOVA ($p < 0.01$), and letters next to the means indicate the results of Tukey's *post hoc* analysis, where different letters represent significant differences between the locations. The highest value for each variable is marked in bold. The explanation of each variable can be found in the Methods.

DOC, dissolved organic carbon; SRP, soluble reactive phosphorus

water samples (ANOSIM $R = 0.053$, $p = 0.216$ for factor surface–hyporheic, Figure 2). With regard to the microbiological activities, differences among locations and among surface water and the interstitial pore water samples were significant (ANOSIM $R = 0.272$, $p < 0.001$ for factor location; ANOSIM $R = 0.412$, $p < 0.001$ for factor surface–hyporheic, Figure 2).

## 3.2 | Changes in water chemistry and microbial activity along hyporheic flow paths

We investigated the temporal variability of the hyporheic zone with drying by plotting the biogeochemical and microbiological parameters for the pool, $HZ_{inf}$ (10 m after the pool) and $HZ_{dw}$ (upwelling location 25 m after the pool) for pre-drought, contraction, transition, and fragmentation separately (Figure 3) and compared increases or decreases with discharge data of the sampling date. For the dry phase, the water level in $HZ_{inf}$ was already below the well bottom.

As shown by the one-way ANOVA (Table 1), the live–dead ratio was higher in the hyporheic zone than in the pool. With lower discharge and longer water residence time, the live–dead ratio decreased to half of the initial values in $HZ_{inf}$ but achieved values of around 0.7 in $HZ_{dw}$ (significant increase along hyporheic flowpaths with lower discharge, Table 2). Extracellular enzyme activities were

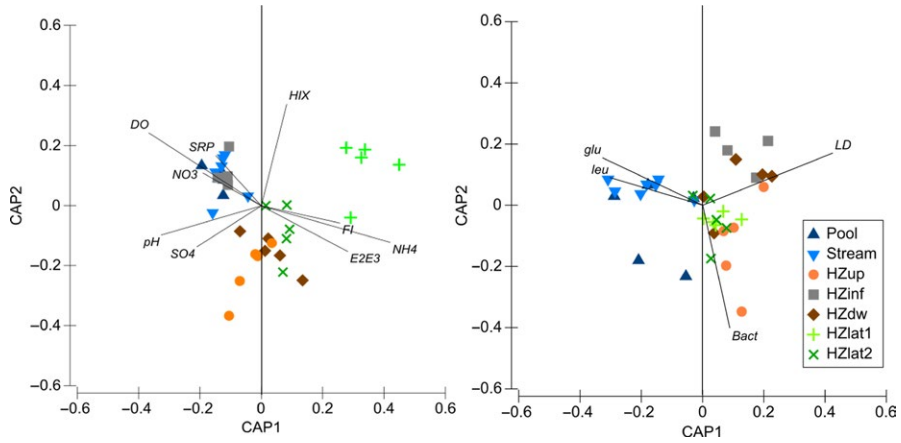


**FIGURE 2** Canonical analysis of principal components (CAP) with location as a factor for chemical variables (left panel) with an overall correct prediction rate of 53% ($m = 9$, $p < 0.001$) and microbiological variables (right panel) with an overall correct prediction rate of 53% ($m = 4$, $p < 0.001$). Vector overlay are Spearman correlations of variables with canonical axes are shown if $|r| > 0.40$. Bact, bacterial cell concentration; DO, dissolved oxygen; E2E3, absorbance ratio; FI, fluorescence index; glu, β-glucosidase; HIX, humification index.; LD, live–dead ratio; leu, leucine aminopeptidase; phos, phosphatase; SRP, soluble reactive phosphorus [Colour figure can be viewed at wileyonlinelibrary.com]

generally lower in $HZ_{inf}$ compared to the pool, but phosphatase and β-glucosidase recovered along the hyporheic flow paths. Generally, these extracellular enzyme activities decreased in the hyporheic zone with longer water residence times and during fragmentation they were nearly undetectable for both hyporheic zone locations (significant for phosphatase, Table 2, Figure 3). Only leucine aminopeptidase showed maximum values in $HZ_{dw}$ during the transition phase, which was when water residence time already exceeded a day. The value of 0.84 nmol $L^{-1}$ $hr^{-1}$ measured this day represents three times the mean value in $HZ_{dw}$ over the whole sampling period. During the transition phase, a peak of bacterial cell concentration of $2.3 \times 10^6$ cells $ml^{-1}$, which is twice the mean bacterial cell concentration of $HZ_{dw}$, was also detected.

The change in concentrations between the pool and $HZ_{dw}$ revealed that the hyporheic zone acted as a sink for dissolved oxygen and both as a sink and a source, for DOC and inorganic nutrients. During contraction, anoxic conditions were detected at night time in $HZ_{dw}$, but still the dissolved oxygen concentration would recover to values above 0.5 mg/L during the day (data not shown). When water residence time exceeded 1 day, the dissolved oxygen was completely consumed in $HZ_{dw}$ at any time of the day. In general, DOC was retained in the hyporheic zone, only interrupted by DOC pulses from $HZ_{inf}$ during the transition phase and from $HZ_{dw}$ during fragmentation. Conversely, SRP and $NO_3$ concentrations always increased when surface water entered the hyporheic zone at $HZ_{inf}$. This increase between pool and $HZ_{inf}$ was higher with longer water residence time and lower discharge (significant for SRP, Table 2), leading to twice the SRP concentration and five times the $NO_3$ concentration of the pool during fragmentation. Between $HZ_{inf}$ and $HZ_{dw}$, SRP concentrations decreased back to pool concentrations. The same applied to $NO_3$ (significantly more decrease with lower discharge, Table 2), but the magnitude of this decrease was not sufficient to remove all the $NO_3$ produced at $HZ_{inf}$. Overall, the $NO_3$ concentration increased by 260%, 230%, and 59% between the pool and $HZ_{dw}$, during pre-drought, contraction, and the transition phases, respectively. Conversely, during fragmentation, the $NO_3$ concentration decreased by 35% between pool and $HZ_{dw}$, even though the concentration was highest in $HZ_{inf}$ during this phase. Contrariwise, $NH_4$ concentrations were lowest at $HZ_{inf}$ and increased along hyporheic flow paths with a peak in $HZ_{dw}$ during the transition phase.

Three optical indices represent how DOM quality changed between the pool and $HZ_{dw}$: $E_2E_3$ increased along hyporheic flow paths, but the magnitude of this increase was not associated with water residence time. The fluorescence index did not show any change between $HZ_{inf}$ and the pool, but clearly increased between $HZ_{inf}$ and $HZ_{dw}$. The humification index showed a similar pattern as the inorganic nutrients, whereby this index increased between the pool and $HZ_{inf}$, but decreased between $HZ_{inf}$ and $HZ_{dw}$. In line with the pattern of the inorganic nutrients, the increase/decrease sequence of humification index showed higher magnitudes with higher water residence time.

### 3.3 | Chemical constraints on microbial activity

We explored the relationships between environmental variables and microbial activity with an RDA (Figure 4). The first two axes were significant ($p < 0.001$), whereby the first axis explained 16% and the second axis 16% of the variation. Out of the 14 environmental variables, six showed a high correlation with the first two RDA axes, namely dissolved oxygen, $NO_3$, SRP, pH, $NH_4$, and $E_2E_3$ ratio (all $p < 0.05$). The $E_2E_3$ absorbance ratio loaded negatively on the first axis and plotted together with the live–dead ratio. This was in contrast to dissolved oxygen concentration, which loaded positively on the first axis and was related to leucine aminopeptidase and β-glucosidase. The second axis separated SRP, $NO_3$, and pH loading positive, from $E_2E_3$ ratio and $NH_4$ that were loading negatively. The $E_2E_3$ ratio and $NH_4$ concentration were related to bacterial cell concentration.

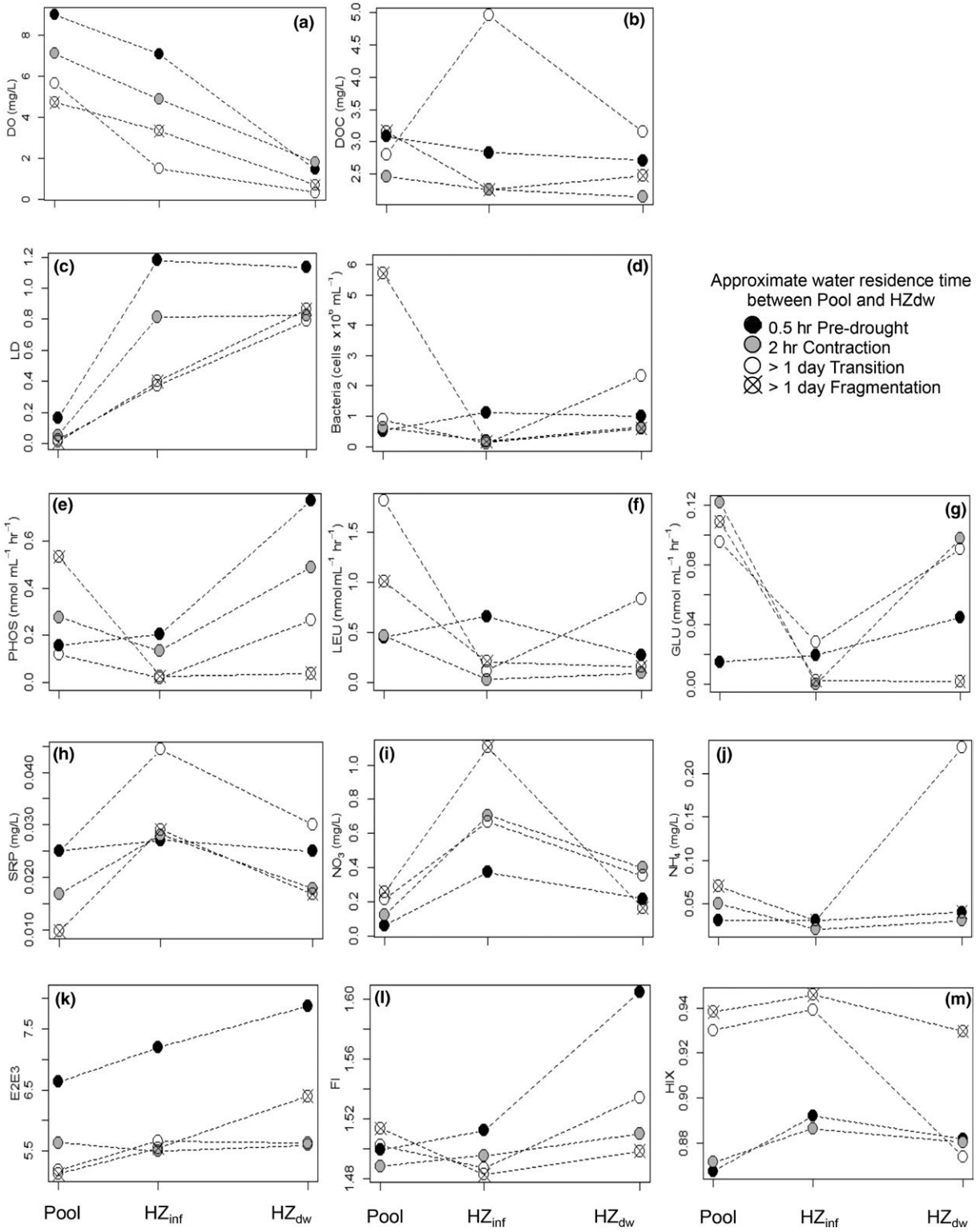


**FIGURE 3** Chemical and microbiological variables for the locations pool, $HZ_{inf}$ and $HZ_{dw}$ during pre-drought, contraction, transition and fragmentation. (a) Dissolved oxygen, (b) dissolved organic carbon, (c) live–dead ratio, (d) bacterial cell concentration, (e) phosphatase, (f) leucine-aminopeptidase, (g) β-glucosidase, (h) soluble reactive phosphorus, (i) nitrate, (j) ammonium, (k) E2E3 absorbance ratio, (l) fluorescence index, (m) humification index

The scores of the RDA showed that the first axis divided surface (plotting positively) from hyporheic water samples (plotting negatively). The isolines (smoothed) mark the five samplings performed during the different phases of the drying period and therefore indicate that the second axis reflects the changes in time. Both, surface and subsurface water samples shifted during the drying period

**TABLE 2** Percentage (%) difference between Pool and $HZ_{inf}$ (infiltration surface water) and between $HZ_{inf}$ and $HZ_{dw}$ (upwelling subsurface)

| | Concentration difference in infiltration surface water | | | | | | Concentration difference in upwelling subsurface | | | | | |
|---|---|---|---|---|---|---|---|---|---|---|---|---|
| **Sampling** | **Pre-drought** | **Con-traction** | **Transition** | **Fragmentation** | **Spearman ρ** | ***p*-value** | **Pre-drought** | **Con-traction** | **Transition** | **Fragmentation** | **Spearman ρ** | ***p*-value** |
| Chemical changes (%) | | | | | | | | | | | | |
| DOC | −8 | −8 | +77 | −29 | 0.32 | 0.68 | −4 | −5 | −36 | +10 | −0.2 | 0.8 |
| Dissolved oxygen | **−21** | **−31** | **−74** | **−29** | **0.4** | **0.6** | **−80** | **−63** | **−79** | **−79** | **−0.32** | **0.68** |
| $NO_3$− | **+516** | **+468** | **+207** | **+327** | **0.8** | **0.2** | −42 | −44 | −47 | −85 | 1 | <0.05 |
| $NH_4$− | 0 | −60 | 0 | −57 | 0.21 | 0.79 | +33 | +50 | +667 | +33 | −0.1 | 0.89 |
| SRP | +8 | +67 | +77 | +199 | −1 | <0.05 | −8 | −36 | −32 | −42 | 0.8 | 0.2 |
| $E_2E_3$ | +8 | **−2** | +9 | +8 | −0.32 | 0.68 | +9 | +2 | **−1** | +15 | −0.2 | 0.8 |
| Humification Index | **+3** | **+2** | **+1** | **+1** | **0.95** | **0.05** | −1 | −1 | −7 | −2 | 0.74 | 0.26 |
| Fluorescence Index | +1 | +1 | **−1** | −2 | 0.95 | 0.05 | +6 | +1 | +3 | +1 | 0.63 | 0.37 |
| Microbial changes (%) | | | | | | | | | | | | |
| live–dead-ratio | **+624** | **+1,474** | **+1,491** | **+4,482** | **−1** | **<0.05** | −4 | +2 | +112 | +117 | −1 | <0.05 |
| Bacterial cell concentration | +113 | −71 | −89 | −97 | 1 | <0.05 | −11 | +251 | +2,261 | +279 | −0.8 | 0.2 |
| β-glucosidase | +29 | −100 | −71 | −98 | 0.4 | 0.6 | +130 | +Inf | +222 | −22 | | |
| Phosphatase | +29 | −52 | −84 | −95 | 1 | <0.05 | +277 | +263 | +1,272 | +50 | 0.4 | 0.6 |
| Leucine-aminopeptidase | +48 | −93 | −93 | −79 | 0.32 | 0.68 | −59 | +192 | +593 | −25 | −0.4 | 0.6 |

| **Maximum and minimum values of the sampling day in $HZ_{dw}$** | | | | |
|---|---|---|---|---|
| | **Pre-drought** | **Contraction** | **Transition** | **Fragmentation** |
| Temperature, °C | 25.4–16.8 | 21.8–17.8 | 21.6–20.9 | 21.2–20.8 |
| Dissolved oxygen, mg/L | 4.89–1.10 | 1.68–0.33 | 0.33–0.30 | 0.33–0.31 |
| Discharge, L/s | 6 | 1.44 | 0.07 | 0.05 |

Negative values indicate decrease and positive values indicate increase. The outcome of the Spearman rank correlation test is presented with Spearman rho and *p*-values testing the correlation between percentage increases and decreases. A negative rho indicates an increase with drying, hence lower discharge, and a positive rho indicates a decrease with drying. If numbers are bold, there was a significant difference between the two locations along all four samplings (paired Student *t* test significant at $p < 0.05$). Rows on the bottom show temperature and oxygen ranges of sampling dates continuously measured at $HZ_{dw}$ and the discharge measured at the outlet of the pool on the same sampling date. The values from pre-drought sampling refer to a date 8 days after the actual sampling date due to battery failure of the same day.

DOC, dissolved organic carbon; SRP, soluble reactive phosphorus

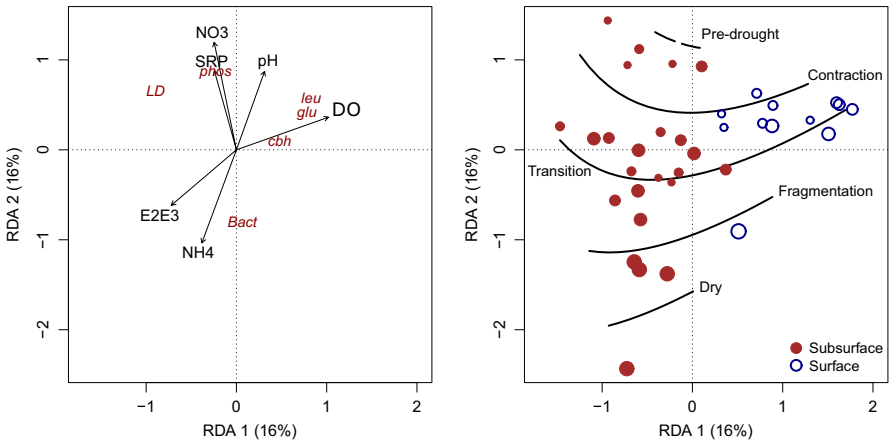


**FIGURE 4** Redundancy analysis (RDA) with biological data from wells fitted with chemical data, on the left only constrained variables are shown with black arrows, which had a significant correlation with RDA axes ($p < 0.05$). Unconstrained variables are shown in dark red/italic. The right panel shows samples distributed in the RDA space with colours indicating subsurface versus surface. The isolines represent samplings phases and the size of the symbols increase with time (drier). DO, dissolved oxygen; LD, live–dead ratio; bact, bacterial cell concentration; phos, phosphatase; leu, leucine aminopeptidase; glu, β-glucosidase; cbh, cellobiohydrolase; SRP, soluble reactive phosphorus; E2E3, absorbance ratio [Colour figure can be viewed at wileyonlinelibrary.com]

towards lower SRP and $NO_3$ concentrations and lower pH, but higher $NH_4$ concentration. This shift was related to a lower live–dead ratio and lower phosphatase, but higher bacterial cell concentration.

## 4 | DISCUSSION

### 4.1 | Microbial activity and biogeochemistry across the surface–hyporheic interface in an intermittent system

We hypothesised that we would find a different nutrient status and DOM availability in the surface waters versus the interstitial pore waters. However, the surface locations did not separate from the hyporheic locations based on these characteristics but based on differences in extracellular enzyme activities and living bacteria abundance. The water in the hyporheic zone of the main channel originated exclusively from the surface water during the study period, but offered a habitat (depth, solid surfaces) for microbial activity that was similar to the lateral sandbanks that represented a mixture of stream water and hillslope runoff. This situation was reflected in our results as follows: $HZ_{inf}$, the location where surface water infiltrated into the hyporheic zone, showed a similar chemical composition as the surface waters, especially regarding the concentrations of dissolved oxygen and $NO_3$. By contrast, the optical indices for DOM in $HZ_{up}$ and $HZ_{dw}$ pointed towards a close relationship of DOM quality and the length of hyporheic flow paths. The chemical composition of the hyporheic zone is typically characterised by lower dissolved oxygen concentrations compared to the surface water and $HZ_{inf}$, as well as in a lower humification degree of the DOM than all other sampling locations, including the wells of the lateral sandbanks.

Conversely, the microbiological variables changed immediately once the water has entered the hyporheic zone, since all interstitial pore water samples showed a clear division from the surface waters (Figure 2). Hence, we suggest a delay between the change in microbial activity that occurs immediately once the water enters the hyporheic zone and the chemical response observed along the hyporheic flow paths.

Very few studies have compared extracellular enzyme activities and bacterial cell concentration in surface and interstitial pore water of natural stream ecosystems (e.g., Ann, 2015; Romaní, Vázquez, & Butturini, 2006). The extracellular enzyme activities β-glucosidase and leucine aminopeptidase from Fuirosos stream surface water in spring season during well-established baseflow connection were twice the maximum values of this study (Ylla et al., 2010). Only right before streambed desiccation, when nearby groundwater did not supply the stream anymore, were the values similarly low. Furthermore, Romaní et al. (2006) report leucine aminopeptidase values in both surface and riparian groundwaters that were even 10-fold higher during a flooding episode in fall ($Q = 400$ L/s). In the literature, we only found comparably low extracellular enzyme activities reported from the larger Tordera River during low flow phase in July (Ann, 2015). Several studies report a close connection between extracellular enzyme activities and DOM availability from different aquatic environments (Baltar, Morán, & Lønborg, 2017; Sabater & Romani, 1996; Ylla, Sanpera-Calbet, Muñoz, Romaní, & Sabater, 2011). In this context, photo-oxidised DOM could either be less labile to bacterial metabolism if amino acids were destroyed (Amado, Cotner, Cory, Edhlund, & McNeill, 2015) or extracellular enzyme activities themselves can be photodegraded in the surface waters due to the shallow water level (Dieter, Frindte, Krüger, & Wurzbacher, 2013; Fernández, Siñeriz, & Farías, 2006). Additionally, leucine aminopeptidase exhibits a very narrow pH range around 7.5 as optimal (Cunha et al., 2010). The pH was mostly below 7, because the low buffering capacity of the water in the granitic catchment favours acidic conditions when humic acids are abundant. Hence, DOM quality could have affected the occurrence of extracellular

enzyme activities directly via DOM reactivity or indirectly by decreasing the pH.

## 4.2 | Linking chemical characteristics and microbial activities during drying: The hyporheic zone as a biogeochemical hot spot

### 4.2.1 | Nutrient retention and DOM mineralisation in the hyporheic zone

Drying and its consequences, such as disconnection of flow paths laterally and longitudinally, as well as longer water residence times (Fisher, Grimm, Martí, & Gómez, 1998; Harvey, Conklin, & Koelsch, 2003) provoked a decrease in SRP and $NO_3$ concentrations that is also observed in other studies from intermittent streams (Bernal & Sabater, 2012; Martí, Grimm, & Fisher, 1997; von Schiller et al., 2008). Additionally, in intermittent streams, the absence of surface flow can involve the diffusion of oxygen into the pore space of the hyporheic zone that triggers ammonia oxidation (Merbt et al., 2016). Both nitrification preceding denitrification in the hyporheic zone increase with water residence times (Zarnetske, Haggerty, Wondzell, & Baker, 2011a). We observed $NO_3$ removal of up to 0.21 mg-N/L during fragmentation between $HZ_{inf}$ and $HZ_{dw}$ when water residence time exceeded a day.

Labile DOC can additionally enhance hyporheic denitrification, with rates of up to 0.37 mg-N/L in 10 hr (Zarnetske, Haggerty, Wondzell, & Baker, 2011b), which is higher but still of a similar magnitude as found in this study. Conversely, DOM infiltrating with the surface water showed a high humification degree in $HZ_{inf}$, in line with high nitrification rates reported when recalcitrant DOM is abundant (Strauss & Lamberti, 2002). However, the DOM quality was improving along hyporheic flow paths, as shown by decreasing humification, but increasing fluorescence index (autochthonous) and $E_2E_3$ (smaller molecules) values. The fluorescence index values showed similar dynamics as βglucosidase, an extracellular enzyme activity that is reported to correlate with autochthonous DOM availability (Freixa, Ejarque, et al., 2016; Proia et al., 2016) and higher $pCO_2$ levels (Grossart, Allgaier, Passow, & Riebesell, 2006). It should be mentioned that humic-like DOM can also be preferentially sorbed to the hyporheic sediments, although we suggest that this might have played a minor role due to the coarse nature of the sediment body of this study (low silt content, no clay fractions in the catchment (Juhna, Klavins, & Eglite, 2003)). Furthermore, the dynamics of β-glucosidase, a drop at $HZ_{inf}$, and an increase in $HZ_{dw}$, are consistent with the DOM retention and the $pCO_2$ release that occurred in this hyporheic zone reach (data in Table S2). DOM derived from surface water can fuel hyporheic metabolism (Clinton, Edwards, & Findlay, 2010), but DOM can also be derived from particulate organic matter, extracellular enzymes or released during anabolic processes in the hyporheic zone (Burrows et al., 2017; Stegen et al., 2016). Fischer et al. (2002) suggested that the cycling of these autochthonous DOM fractions might be faster and consequently their contribution to bacterial metabolism would be higher than inferred from the apparent DOM retention.

Moreover, bacterial cell concentration increased in all sampling locations with drying that is in contrast to continuous flow column experiments, where bacterial cell concentration rapidly decreased with depth (Perujo et al., 2017). Conversely, a reported increase in bacterial cell concentration in the interstitial pore water of a sediment desiccation laboratory experiment (Pohlon, Fandino, & Marxsen, 2013), suggests that microbial activity in intermittent streams follows a different distribution pattern of microbial activity than their perennial counterparts. Furthermore, the results of this laboratory experiment indicated a community shift towards bacteria that are more efficient in carbon and nutrient acquisition (Pohlon et al., 2013). This described community shift could also explain the decrease in nutrient concentrations and apparent DOM molecular size.

### 4.2.2 | The hyporheic zone as a refuge

The hyporheic zone appeared to have acted as a refuge for the bacteria during the drying period of the stream as shown by higher live–dead ratio of subsurface waters compared to the surface water. The sediment desiccation of intermittent rivers is reported to drastically reduce living bacteria when experimentally tested in mesocosms (Amalfitano et al., 2008). However, we suggest that natural streams and rivers often maintain deeper, water-saturated layers of the hyporheic zone as a refuge for microbial activity during drought as suggested by Romaní et al. (2013). We found significantly higher live–dead ratios in the interstitial pore water compared to surface water that points towards this survival mechanism of bacteria and is further evidenced by the increase of the live–dead ratio along the hyporheic flow path between $HZ_{inf}$ and $HZ_{dw}$. Similarly, the bacterial community in the hyporheic zone (at 10 cm depth) of Fuirosos showed higher resistance to drying than the upper layers of sandy sediment cores (Timoner, Borrego, Acuña, & Sabater, 2014). Furthermore, Ann (2015) reports higher extracellular enzyme activities in interstitial water of the Tordera River with absence of surface flow from sediment depths similar to those of this study (−30 to −50 cm). Concerning the resistance mechanisms of microbial metabolism during drought, there is a paucity of studies reporting live–dead ratios and bacterial cell concentration in interstitial pore water. This would be particularly of interest, as prokaryotes are able to travel greater distances and deeper into the hyporheic zone with the water flow, because of their ubiquitous nature (Febria et al., 2012; Peralta-Maraver, Reiss, & Robertson, 2018; Romaní et al., 2017). In this sense, prokaryotes might have a survival advantage compared to larger microbes that makes them the essential actors of nutrient retention and DOM mineralisation in intermittent streams as well as other environments with fluctuating water levels (Goldman et al., 2017; Stegen et al., 2016). Hence, there might be an underestimation of bacterial survival of droughts and hot spots in the hyporheic zone that can show enhanced carbon turnover rates (Gómez-Gener et al., 2016;

Ylla et al., 2010). This idea is further corroborated by the much lower microbial activity that we found in the interstitial pore water in October when the fluvial continuum had re-established (data shown in Table S1). Still, we have to acknowledge the fact that the number of observations in this study is small and further studies are needed to fully understand the hyporheic zone as a refuge for microbial activity. For example, microbial metabolism was shown to be affected by the hydraulic conductivity of the hyporheic zone (Mendoza-Lera & Datry, 2017). Further, we suggest comparing intermittent streams with previously perennial streams or to test different water depths to understand how deep the prokaryotes can migrate. Conclusively, our results emphasise the importance of the hyporheic zone during drought: not just that remaining water-saturated locations are biogeochemical hot spots during drought that act as DOM and nutrient sinks, but they can also provide a refuge for microbial activity that can explain enhanced DOM and nutrient turnover rates upon rewetting.

## ACKNOWLEDGMENTS

We thank M. A. Gallegos and P. Rodrigo for field and laboratory assistance. We are grateful for the helpful comments of four anonymous reviewers that improved the manuscript. This study was funded by European Union's Seventh Framework Marie Curie training project INTERFACES (grant agreement no 607150) and was partly supported by the project GLOBAQUA (603629-ENV-6.2.1). A.H., A.B., and F.S. are members of the research group ForeSTream (2014SGR949).

## CONFLICT OF INTEREST

The authors declare no conflict of interest.

## ORCID

*Astrid Harjung* https://orcid.org/0000-0002-6129-8352

## REFERENCES

Amado, A. M., Cotner, J. B., Cory, R. M., Edhlund, B. L., & McNeill, K. (2015). Disentangling the interactions between photochemical and bacterial degradation of dissolved organic matter: Amino acids play a central role. *Microbial Ecology*, *69*, 554–566. https://doi.org/10.1007/s00248-014-0512-4

Amalfitano, S., & Fazi, S. (2008). Recovery and quantification of bacterial cells associated with streambed sediments. *Journal of Microbiological Methods*, *75*, 237–243. https://doi.org/10.1016/j.mimet.2008.06.004

Amalfitano, S., Fazi, S., Zoppini, A., Barra Caracciolo, A., Grenni, P., & Puddu, A. (2008). Responses of benthic bacteria to experimental drying in sediments from Mediterranean temporary rivers. *Microbial Ecology*, *55*, 270–279. https://doi.org/10.1007/s00248-007-9274-6

Anderson, M. J., Gorley, R. N., & Clarke, K. R. (2008). *PERMANOVA+ for PRIMER: Guide to software and statistical methods* (pp. 1–214). Plymouth, UK: PRIMER-E, Ltd.

Anderson, M. J., & Willis, T. (2012). Canonical analysis of principal coordinates: A useful method of constrained ordination for ecology. *Ecology*, *84*, 511–525.

Anesio, A. M., Granéli, W., Aiken, G. R., Kieber, D. J., & Mopper, K. (2005). Effect of humic substance photodegradation on bacterial growth and respiration in lake water. *Applied and Environmental Microbiology*, *71*, 6267–6275. https://doi.org/10.1128/aem.71.10.6267-6275.2005

Ann, V. (2015). Linking river sediment physical properties to biofilm biomass and activity. PhD thesis. Universitat de Girona.

Arce, M. I., del Mar Sánchez-Montoya, M., Rosario Vidal-Abarca, M., Suárez, M. L., & Gómez, R. (2014). Implications of flow intermittency on sediment nitrogen availability and processing rates in a Mediterranean headwater stream. *Aquatic Sciences*, *76*, 173–186. https://doi.org/10.1007/s00027-013-0327-2

Artigas, J., Romaní, A. M., Gaudes, A., Muñoz, I., & Sabater, S. (2009). Organic matter availability structures microbial biomass and activity in a Mediterranean stream. *Freshwater Biology*, *54*, 2025–2036. https://doi.org/10.1111/j.1365-2427.2008.02140.x

Baltar, F., Morán, X. A. G., & Lønborg, C. (2017). Warming and organic matter sources impact the proportion of dissolved to total activities in marine extracellular enzymatic rates. *Biogeochemistry*, *133*, 307–316. https://doi.org/10.1007/s10533-017-0334-9

Bernal, S., & Sabater, F. (2012). Changes in discharge and solute dynamics between hillslope and valley-bottom intermittent streams. *Hydrology and Earth System Sciences*, *16*, 1595–1605. https://doi.org/10.5194/hess-16-1595-2012

Boulos, L., Prévost, M., Barbeau, B., Coallier, J., & Desjardins, R. (1999). LIVE/DEAD ® Bac Light E : Application of a new rapid staining method for direct enumeration of viable and total bacteria in drinking water. *Journal of Microbiological Methods*, *37*, 77–86. https://doi.org/10.1016/s0167-7012(99)00048-2

Boulton, A. J., Datry, T., Kasahara, T., Mutz, M., & Stanford, J. A. (2010). Ecology and management of the hyporheic zone: Stream–groundwater interactions of running waters and their floodplains. *Journal of the North American Benthological Society*, *29*, 26–40. https://doi.org/10.1899/08-017.1

Boulton, A. J., Findlay, S., Marmonier, P., Stanley, E. H., & Valett, H. M. (1998). The functional significance of the hyporheic zone in streams and rivers. *Annual Review of Ecology and Systematics*, *29*, 59–81. https://doi.org/10.1146/annurev.ecolsys.29.1.59

Burrows, R. M., Rutlidge, H., Bond, N. R., Eberhard, S. M., Auhl, A., Andersen, M. S., … Kennard, M. J. (2017). High rates of organic carbon processing in the hyporheic zone of intermittent streams. *Scientific Reports*, *7*, 13198. https://doi.org/10.1038/s41598-017-12957-5

Butturini, A., Bernal, S., Hellin, C., Nin, E., Rivero, L., Sabater, S., & Sabater, F. (2003). Influences of the stream groundwater hydrology on nitrate concentration in unsaturated riparian area bounded by an intermittent Mediterranean stream. *Water Resources Research*, *39*, 1110. https://doi.org/10.1029/2001WR001260, 4

Butturini, A., Bernal, S., Sabater, S., & Sabater, F. (2002). The influence of riparian-hyporheic zone on the hydrological responses in an intermittent stream. *Hydrology and Earth System Sciences*, *6*, 515–526. https://doi.org/10.5194/hess-6-515-2002

Chafiq, M., Gibert, J., & Claret, C. (1999). Interactions among sediments, organic matter, and microbial activity in the hyporheic zone of an intermittent stream. *Canadian Journal of Fisheries and Aquatic Sciences*, *56*, 487–495. https://doi.org/10.1139/f98-208

Clinton, S. M., Edwards, R. T., & Findlay, S. E. G. (2010). Exoenzyme activities as indicators of dissolved organic matter composition in the hyporheic zone of a floodplain river. *Freshwater Biology*, *55*, 1603–1615. https://doi.org/10.1111/j.1365-2427.2009.02383.x

Cory, R. M., & McKnight, D. M. (2005). Fluorescence spectroscopy reveals ubiquitous presence of oxidized and reduced quinones in

dissolved organic matter. *Environmental Science & Technology*, *39*, 8142–8149. https://doi.org/10.1021/es0506962

Cunha, A., Almeida, A., Coelho, F. J. R. C., Gomes, N. C. M., Oliveira, V., & Santos, A. L. (2010). Bacterial extracellular enzymatic activity in globally changing aquatic ecosystems. *Current Research, Technology and Education Topics in Applied Microbiology and Microbial Biotechnology*, 124–135.

Danczak, R. E., Sawyer, A. H., Williams, K. H., Stegen, J. C., Hobson, C., & Wilkins, M. J. (2016). Seasonal hyporheic dynamics control coupled microbiology and geochemistry in Colorado River sediments. *Journal of Geophysical Research: Biogeosciences*, *121*, 2976–2987.

Dieter, D., Frindte, K., Krüger, A., & Wurzbacher, C. (2013). Preconditioning of leaves by solar radiation and anoxia affects microbial colonisation and rate of leaf mass loss in an intermittent stream. *Freshwater Biology*, *58*, 1918–1931. https://doi.org/10.1111/fwb.12180

Edwardson, K. J., Bowden, W. B., Dahm, C., & Morrice, J. (2003). The hydraulic characteristics and geochemistry of hyporheic and parafluvial zones in Arctic tundra streams, north slope, Alaska. *Advances in Water Resources*, *26*, 907–923. https://doi.org/10.1016/s0309-1708(03)00078-2

Eiler, A., Langenheder, S., Bertilsson, S., & Tranvik, L. J. (2003). Heterotrophic bacterial growth efficiency and community structure at different natural organic carbon concentrations. *Applied and Environmental Microbiology*, *69*, 3701–3709. https://doi.org/10.1128/aem.69.7.3701-3709.2003

Farjalla, V. F., Marinho, C. C., Faria, B. M., Amado, A. M., Esteves, F. D. A., Bozelli, R. L., & Giroldo, D. (2009). Synergy of fresh and accumulated organic matter to bacterial growth. *Microbial Ecology*, *57*, 657–666. https://doi.org/10.1007/s00248-008-9466-8

Febria, C. M., Beddoes, P., Fulthorpe, R. R., & Williams, D. D. (2012). Bacterial community dynamics in the hyporheic zone of an intermittent stream. *The ISME Journal*, *6*, 1078–1088. https://doi.org/10.1038/ismej.2011.173

Fernández, Zenoff. V., Siñeriz, F., & Farías, M. E. (2006). Diverse responses to UV-B radiation and repair mechanisms of bacteria isolated from high-altitude aquatic environments. *Applied and Environmental Microbiology*, *72*, 7857–7863. https://doi.org/10.1128/aem.01333-06

Fischer, H., Sachse, A., Steinberg, C. E. W., & Pusch, M. (2002). Differential retention and utilization of dissolved organic carbon by bacteria in river sediments. *Limnology and Oceanography*, *47*, 1702–1711. https://doi.org/10.4319/lo.2002.47.6.1702

Fisher, S. G., Grimm, N. B., Martí, E., & Gómez, R. (1998). Hierarchy, spatial configuration, and nutrient cycling in a desert stream. *Austral Ecology*, *23*, 41–52. https://doi.org/10.1111/j.1442-9993.1998.tb00704.x

Freixa, A., Ejarque, E., Crognale, S., Amalfitano, S., Fazi, S., Butturini, A., & Romaní, A. M. (2016). Sediment microbial communities rely on different dissolved organic matter sources along a Mediterranean river continuum. *Limnology and Oceanography*, *61*, 1389–1405. https://doi.org/10.1002/lno.10308

Freixa, A., Rubol, S., Carles-Brangarí, A., Fernàndez-Garcia, D., Butturini, A., Sanchez-Vila, X., & Romaní, A. M. (2016). The effects of sediment depth and oxygen concentration on the use of organic matter: An experimental study using an infiltration sediment tank. *Science of the Total Environment*, *540*, 20–31. https://doi.org/10.1016/j.scitotenv.2015.04.007

Gardecki, J. A., & Maroncelli, M. (1998). Set of secondary emission standards for calibration of the spectral responsivity in emission spectroscopy. *Applied Spectroscopy*, *52*, 1179–1189. https://doi.org/10.1366/0003702981945192

Goldman, A. E., Graham, E. B., Crump, A. R., Kennedy, D. W., Romero, E. B., Anderson, C. G., … Stegen, J. C. (2017). Biogeochemical cycling at the aquatic-terrestrial interface is linked to parafluvial hyporheic zone inundation history. *Biogeosciences*, *14*, 4229–4241. https://doi.org/10.5194/bg-14-4229-2017

Goletz, C., Wagner, M., Grübel, A., Schmidt, W., Korf, N., & Werner, P. (2011). Standardization of fluorescence excitation–emission-matrices in aquatic milieu. *Talanta*, *85*, 650–656. https://doi.org/10.1016/j.talanta.2011.04.045

Gómez, R., García, V., Vidal-Abarca, R., & Suárez, L. (2009). Effect of intermittency on N spatial variability in an arid Mediterranean stream. *Journal of the North American Benthological Society*, *28*, 572–583. https://doi.org/10.1899/09-016.1

Gómez-Gener, L., Obrador, B., Marcé, R., Acuña, V., Catalán, N., Casas-Ruiz, J. P., … von Schiller, D. (2016). When water vanishes: Magnitude and regulation of carbon dioxide emissions from dry temporary streams. *Ecosystems*, *19*, 710–723. https://doi.org/10.1007/s10021-016-9963-4

Grossart, H. P., Allgaier, M., Passow, U., & Riebesell, U. (2006). Testing the effect of $CO_2$ concentration on the dynamics of marine heterotrophic bacterioplankton. *Limnology and Oceanography*, *51*, 1–11. https://doi.org/10.4319/lo.2006.51.1.0001

Hall, R. O., & Tank, J. L. (2003). Ecosystem metabolism controls nitrogen uptake in streams in Grand Teton National Park, Wyoming. *Limnology and Oceanography*, *48*, 1120–1128. https://doi.org/10.4319/lo.2003.48.3.1120

Harjung, A., Sabater, F., & Butturini, A. (2017). Hydrological connectivity drives dissolved organic matter processing in an intermittent stream. *Limnologica - Ecology and Management of Inland Waters*, *68*, 71–81.

Harvey, J. W., Böhlke, J. K., Voytek, M. A., Scott, D., & Tobias, C. R. (2013). Hyporheic zone denitrification: Controls on effective reaction depth and contribution to whole-stream mass balance. *Water Resources Research*, *49*, 6298–6316. https://doi.org/10.1002/wrcr.20492

Harvey, J. W., Conklin, M. H., & Koelsch, R. S. (2003). Predicting changes in hydrologic retention in an evolving semi-arid alluvial stream. *Advances in Water Resources*, *26*, 939–950. https://doi.org/10.1016/s0309-1708(03)00085-x

Helms, J. R., Stubbins, A., Ritchie, J. D., Minor, E. C., Kieber, D. J., & Mopper, K. (2008). Absorption spectral slopes and slope ratios as indicators of molecular weight, source, and photobleaching of chromophoric dissolved organic matter. *Limnology and Oceanography*, *53*, 955–969. https://doi.org/10.4319/lo.2008.53.3.0955

Huguet, A., Vacher, L., Relexans, S., Saubusse, S., Froidefond, J. M., & Parlanti, E. (2009). Properties of fluorescent dissolved organic matter in the Gironde Estuary. *Organic Geochemistry*, *40*, 706–719. https://doi.org/10.1016/j.orggeochem.2009.03.002

Juhna, T., Klavins, M., & Eglite, L. (2003). Sorption of humic substances on aquifer material at artificial recharge of groundwater. *Chemosphere*, *51*, 861–868. https://doi.org/10.1016/s0045-6535(03)00108-5

Keeney, D. R., & Nelson, D. W. (1982) Nitrogen-inorganic forms. In A. L. Page, D. R. Keeney, D. E. Baker, R. H. Miller, R. J. Ellis & J. D. Rhoades (Eds.), *Methods of soil analysis: Part 2* (pp. 643–698). Madison: American Society of Agronomy.

Krause, S., Hannah, D. M., Fleckenstein, J. H., Heppell, C. M., Kaeser, D., Pickup, R., … Wood, P. J. (2011). Inter-disciplinary perspectives on processes in the hyporheic zone. *Ecohydrology*, *4*, 481–499. https://doi.org/10.1002/eco.176

Lake, P. S. (2003). Ecological effects of perturbation by drought in flowing waters. *Freshwater Biology*, *48*, 1161–1172. https://doi.org/10.1046/j.1365-2427.2003.01086.x

Lakowicz, J. R. (2006). *Principles of fluorescence spectroscopy* (3rd ed.). New York, NY: Springer. https://doi.org/10.1007/978-0-387-46312-4

Lawaetz, A. J., & Stedmon, C. A. (2008). Fluorescence intensity calibration using the Raman scatter peak of water fluorescence intensity calibration using the Raman scatter peak of water. *Applied Spectroscopy*, *63*, 936–940.

Legendre, P., & Gallagher, E. D. (2001). Ecologically meaningful transformations for ordination of species data. *Oecologia*, *129*, 271–280. https://doi.org/10.1007/s004420100716

Liu, Y., Liu, C., Nelson, W. C., Shi, L., Xu, F., Liu, Y., … Zachara, J. M. (2017). Effect of water chemistry and hydrodynamics on nitrogen transformation activity and microbial community functional potential in hyporheic zone sediment columns. *Environmental Science & Technology*, *51*, 4877–4886. https://doi.org/10.1021/acs.est.6b05018

Martí, E., Grimm, N. B., & Fisher, S. G. (1997). Pre- and post-flood retention efficiency of nitrogen in a Sonoran Desert stream. *Journal of the North American Benthological Society*, *16*, 805–819. https://doi.org/10.2307/1468173

McClain, M. E., Boyer, E. W., Dent, C. L., Gergel, S. E., Grimm, N. B., Groffman, P. M., … Pinay, G. (2003). Biogeochemical hot spots and hot moments at the interface of terrestrial and aquatic ecosystems. *Ecosystems*, *6*, 301–312. https://doi.org/10.1007/s10021-003-0161-9

McKnight, D. M., Boyer, E. W., Westerhoff, P. K., Doran, P. T., Kulbe, T., & Andersen, D. T. (2001). Spectrofluorometric characterization of dissolved organic matter for indication of precursor organic material and aromaticity. *Limnology and Oceanography*, *46*, 38–48. https://doi.org/10.4319/lo.2001.46.1.0038

Medici, C., Butturini, A., Bernal, S., Vázquez, E., Sabater, F., Vélez, J. I., … Francés, F. (2008). Modelling the non-linear hydrological behaviour of a small Mediterranean forested catchment. *Hydrological Processes*, *22*, 3814–3828. https://doi.org/10.1002/hyp.6991

Mendoza-Lera, C., & Datry, T. (2017). Relating hydraulic conductivity and hyporheic zone biogeochemical processing to conserve and restore river ecosystem services. *Science of the Total Environment*, *579*, 1815–1821. https://doi.org/10.1016/j.scitotenv.2016.11.166

Merbt, S. N., Proia, L., Prosser, J. I., Marti, E., Casamayor, E. O., & Von Schiller, D. (2016). Stream drying drives microbial ammonia oxidation and first-flush nitrate export. *Ecology*, *97*, 2192–2198. https://doi.org/10.1002/ecy.1486

Mora-Gómez, J., Duarte, S., Cássio, F., Pascoal, C., & Romaní, A. M. (2018). Microbial decomposition is highly sensitive to leaf litter emersion in a permanent temperate stream. *Science of the Total Environment*, *621*, 486–496. https://doi.org/10.1016/j.scitotenv.2017.11.055

Murphy, J., & Riley, J. P. (1962). A modified single solution method for the determination of phosphate in natural waters. *Analytica Chimica Acta*, *27*, 31–36. https://doi.org/10.1016/s0003-2670(00)88444-5

Naegeli, M. W., & Uehlinger, U. (1997). Contribution of the hyporheic zone to ecosystem metabolism in a prealpine gravel-bed-river. *Journal of the North American Benthological Society*, *16*, 794–804. https://doi.org/10.2307/1468172

Ohno, T. (2002). Fluorescence inner-filtering correction for determining the humification index of dissolved organic matter. *Environmental Science & Technology*, *36*, 742–746. https://doi.org/10.1021/es0155276

Oksanen, J., Blanchet, F. G., Kindt, R., Legendre, P., Minchin, P. R., O'Hara, R. B., & Wagner, H.. (2013). Package 'vegan'. R package ver. 2.0–8, 254.

Pachauri, R. K., Meyer, L., Van Ypersele, J.-P., Brinkman, S., Van Kesteren, L., Leprince-Ringuet, N., & van Boxmeer, F. (2014). *Climate Change 2014 Synthesis Report the Core Writing Team Core Writing Team Technical Support Unit for the Synthesis Report*. IPCC, Geneva, Switzerland.

Peacock, M., Evans, C. D., Fenner, N., Freeman, C., Gough, R., Jones, T. G., & Lebron, I. (2014). UV-visible absorbance spectroscopy as a proxy for peatland dissolved organic carbon (DOC) quantity and quality: Considerations on wavelength and absorbance degradation. *Environmental Science: Processes & Impacts*, *16*, 1445.

Peralta-Maraver, I., Reiss, J., & Robertson, A. L. (2018). Interplay of hydrology, community ecology and pollutant attenuation in the hyporheic zone. *Science of the Total Environment*, *610*(611), 267–275. https://doi.org/10.1016/j.scitotenv.2017.08.036

Perujo, N., Sanchez-Vila, X., Proia, L., & Romaní, A. M. (2017). Interaction between physical heterogeneity and microbial processes in subsurface sediments: A laboratory-scale column experiment. *Environmental Science & Technology*, *51*, 6110–6119. https://doi.org/10.1021/acs.est.6b06506

Pohlon, E., Fandino, A. O., & Marxsen, J. (2013). Bacterial community composition and extracellular enzyme activity in temperate streambed sediment during drying and rewetting. *PLoS ONE*, *8*, e83365. https://doi.org/10.1371/journal.pone.0083365

Proia, L., von Schiller, D., Gutierrez, C., Casas-Ruiz, J. P., Gómez-Gener, L., Marcé, R., & Sabater, S. (2016). Microbial carbon processing along a river discontinuum. *Freshwater Science*, *35*, 1133–1147. https://doi.org/10.1086/689181

Rasilo, T., Hutchins, R. H. S., Ruiz-González, C., & del Giorgio, P. A. (2017). Transport and transformation of soil-derived $CO_2$, $CH_4$ and DOC sustain $CO_2$ supersaturation in small boreal streams. *Science of the Total Environment*, *579*, 902–912. https://doi.org/10.1016/j.scitotenv.2016.10.187

Ratkowsky, D. A. (2016). Choosing the number of principal coordinates when using CAP, the canonical analysis of principal coordinates. *Austral Ecology*, *41*, 842–851. https://doi.org/10.1111/aec.12378

Reardon, J. (1966). *Salicylate method for the quantitative determination of ammonia nitrogen*. Washington, DC: U.S. Patent and Trademark Office.

Romaní, A. M., Amalfitano, S., Artigas, J., Fazi, S., Sabater, S., Timoner, X., … Zoppini, A. (2013). *Microbial biofilm structure and organic matter use in mediterranean streams*. Dordrecht, Netherlands: Springer. https://doi.org/10.1007/s10750-012-1302-y

Romaní, A. M., Chauvet, E., Febria, C., Mora-Gómez, J., Risse-Buhl, U., Timoner, X., … Zeglin, L. (2017). The biota of intermittent rivers and ephemeral streams: Prokaryotes, fungi, and protozoans. In T. Datry, N. Bonada, & A. Boulton (Eds.), *Intermittent rivers and ephemeral streams* (pp. 161–188). New York, NY: Elsevier. https://doi.org/10.1016/b978-0-12-803835-2.00009-7

Romaní, A. M., & Sabater, S. (2000). Influence of algal biomass on extracellular enzyme activity in river biofilms. *Microbial Ecology*, *40*, 16–24. https://doi.org/10.1007/s002480000041

Romaní, A. M., Vázquez, E., & Butturini, A. (2006). Microbial availability and size fractionation of dissolved organic carbon after drought in an intermittent stream: Biogeochemical link across the stream-riparian interface. *Microbial Ecology*, *52*, 501–512. https://doi.org/10.1007/s00248-006-9112-2

Sabater, S., & Romani, A. M. (1996). Metabolic changes associated with biofilm formation in an undisturbed Mediterranean stream. *Hydrobiologia*, *335*, 107–113. https://doi.org/10.1007/bf00015272

von Schiller, D., Martí, E., Riera, J. L., Ribot, M., Argerich, A., Fonollà, P., & Sabate, F. (2008). Inter-annual, annual, and seasonal variation of P and N retention in a perennial and an intermittent stream. *Ecosystems*, *11*, 670–687. https://doi.org/10.1007/s10021-008-9150-3

Stegen, J. C., Fredrickson, J. K., Wilkins, M. J., Konopka, A. E., Nelson, W. C., Arntzen, E. V., … Tfaily, M. (2016). Groundwater–surface water mixing shifts ecological assembly processes and stimulates organic carbon turnover. *Nature Communications*, *7*, 11237. https://doi.org/10.1038/ncomms11237

Storey, R. G., Williams, D. D., & Fulthorpe, R. R. (2004). Nitrogen processing in the hyporheic zone of a pastoral stream. *Biogeochemistry*, *69*, 285–313. https://doi.org/10.1023/b:biog.0000031049.95805.ec

Strauss, E. A., & Lamberti, G. A. (2002). Effect of dissolved organic carbon quality on microbial decomposition and nitrification rates in stream sediments. *Freshwater Biology*, *47*, 65–74. https://doi.org/10.1046/j.1365-2427.2002.00776.x

Timoner, X., Borrego, C. M., Acuña, V., & Sabater, S. (2014). The dynamics of biofilm bacterial communities is driven by flow wax and wane in a temporary stream. *Limnology and Oceanography*, *59*, 2057–2067. https://doi.org/10.4319/lo.2014.59.6.2057

Triska, F. J., Duff, J. H., & Avanzino, R. J. (1990). Influence of exchange flow between the channel and hyporheic zone on nitrate production in a small mountain stream. *Canadian Journal of Fisheries and Aquatic Sciences*, *47*, 2099–2111. https://doi.org/10.1139/f90-235

Vazquez, E., Acuña, V., Artigas, J., Bernal, S., Ejarque, E., Gaudes, A., … Butturin, A. (2013). Fourteen years of hydro-biogeochemical monitoring in a Mediterranean catchment. *Bodenkultur*, *64*, 13–20.

Vázquez, E., Amalfitano, S., Fazi, S., & Butturini, A. (2011). Dissolved organic matter composition in a fragmented Mediterranean fluvial system under severe drought conditions. *Biogeochemistry*, *102*, 59–72. https://doi.org/10.1007/s10533-010-9421-x

Vervier, P., Dobson, M., & Pinay, G. (1993). Role of interaction zones between surface and ground waters in DOC transport and processing: Considerations for river restoration. *Freshwater Biology*, *29*, 275–284. https://doi.org/10.1111/j.1365-2427.1993.tb00763.x

Wagner, K., Bengtsson, M. M., Besemer, K., Sieczko, A., Burns, N. R., Herberg, E. R., & Battin, T. J. (2014). Functional and structural responses of hyporheic biofilms to varying sources of dissolved organic matter. *Applied and Environmental Microbiology*, *80*, 6004–6012. https://doi.org/10.1128/aem.01128-14

Weishaar, J. L., Aiken, G. R., Bergamaschi, B. A., Fram, M. S., Fujii, R., & Mopper, K. (2003). Evaluation of specific ultraviolet absorbance as an indicator of the chemical composition and reactivity of dissolved organic carbon. *Environmental Science & Technology*, *37*, 4702–4708. https://doi.org/10.1021/es030360x

Wondzell, S. M., & Gooseff, M. N. (2013). Geomorphic controls on hyporheic exchange across scales: Watersheds to particles. In J. Shroder & E. Wohl (Eds.), *Treatise on geomorphology* (pp. 203–218). San Diego, California: Academic Press.

Ylla, I., Sanpera-Calbet, I., Muñoz, I., Romaní, A. M., & Sabater, S. (2011). Organic matter characteristics in a Mediterranean stream through amino acid composition: Changes driven by intermittency. *Aquatic Sciences*, *73*, 523–535. https://doi.org/10.1007/s00027-011-0211-x

Ylla, I., Sanpera-Calbet, I., Vázquez, E., Romaní, A. M., Muñoz, I., Butturini, A., & Sabater, S. (2010). Organic matter availability during pre- and post-drought periods in a Mediterranean stream. *Hydrobiologia*, *657*, 217–232. https://doi.org/10.1007/s10750-010-0193-z

Zarnetske, J. P., Haggerty, R., Wondzell, S. M., & Baker, M. A. (2011a). Dynamics of nitrate production and removal as a function of residence time in the hyporheic zone. *Journal of Geophysical Research*, *116*, G01025.

Zarnetske, J. P., Haggerty, R., Wondzell, S. M., & Baker, M. A. (2011b). Labile dissolved organic carbon supply limits hyporheic denitrification. *Journal of Geophysical Research*, *116*, G04036.

Zhu, T., & Dittrich, M. (2016). Carbonate precipitation through microbial activities in natural environment, and their potential in biotechnology: A review. *Frontiers in Bioengineering and Biotechnology*, *4*, 4.

## SUPPORTING INFORMATION

Additional supporting information may be found online in the Supporting Information section at the end of the article.

**How to cite this article:** Harjung A, Perujo N, Butturini A, Romaní AM, Sabater F. Responses of microbial activity in hyporheic pore water to biogeochemical changes in a drying headwater stream. *Freshwater Biol*. 2019;64:735–749. https://doi.org/10.1111/fwb.13258